MicroRNA-129-5p is regulated by choline availability and controls EGF receptor synthesis and neurogenesis in the cerebral cortex

Isis Trujillo-Gonzalez,* Yanyan Wang,*,† Walter B. Friday,* Kasey C. Vickers,‡ Cynthia L. Toth,‡ Lorian Molina-Torres,* Natalia Surzenko,*,§,2 and Steven H. Zeisel*,§,1

*Nutrition Research Institute, University of North Carolina at Chapel Hill, Kannapolis, North Carolina, USA; †Department of Medical Genetics, Third Military Medical University, Chongqing, China; ‡Division of Cardiovascular Medicine, Vanderbilt University School of Medicine, Nashville, Tennessee, USA; and §Department of Nutrition, Gillings School of Global Public Health, University of North Carolina at Chapel Hill, Chapel Hill, North Carolina, USA

ABSTRACT: Choline availability modulates neurogenesis and cerebral cortex development through the regulation of neural progenitor cell (NPC) proliferative and differentiation capacity. In this study, we demonstrated that cortical NPC self-renewal is controlled by choline *via* the expression of a microRNA (miR-129-5p), whose role in the developing brain has not been examined, and which, in turn, inhibits synthesis of the epidermal growth factor receptor (EGFR) protein. Specifically, we found that low choline (LC) availability led to the upregulation of miR-129-5p expression in cortical NPCs *in vitro* and *in vivo*, causing the downregulation of EGFR and thereby disrupting NPC self-renewal and cortical neurogenesis. Furthermore, in response to LC availability, methylation potential (the *S*-adenosylmethionine:*S*-adenosylhomocysteine ratio) in the developing brain was reduced. Restoring methylation potential in LC cortical NPCs led to the re-establishment of normal miR-129-5p expression. We concluded that inhibiting miR-129-5p function and restoring EGFR protein levels *in vivo* is sufficient to reverse LC-induced defects in cortical NPC self-renewal. For the first time, to our knowledge, we have identified the molecular links that explain how a change in the availability of the diet metabolite choline impacts the essential cellular processes underlying brain development.—Trujillo-Gonzalez, I., Wang, Y., Friday, W. B., Vickers, K. C., Toth, C. L., Molina-Torres, L., Surzenko, N., Zeisel, S. H. MicroRNA-129-5p is regulated by choline availability and controls EGF receptor synthesis and neurogenesis in the cerebral cortex. FASEB J. 33, 3601–3612 (2019). www.fasebj.org

KEY WORDS: cortical development · EGFR · maternal nutrition · brain development

Choline is a nutrient that is essential for multiple cellular functions, such as the production of the neurotransmitter acetylcholine and synthesis of betaine—a metabolite involved in the generation of methyl groups that are necessary for DNA, RNA, and protein methylation (1).

Phosphatidylcholine, another choline metabolite, is one of the most abundant components of the cellular membranes (2). The importance of adequate choline (AC) for brain development has been well established (1). If choline availability is increased above adequate in pregnant rodent dams, between d 11 and 17 of gestation, the offspring perform better on memory-related tasks, such as the Morris water maze and radial arm maze, throughout life (3–7). In humans, higher intake of choline during pregnancy is associated with better performance on memory tests in the 7-yr-old children of these mothers (8). On the contrary, an insufficient supply of choline during development increases the risk of neural tube closure defects (9) and leads to aberrant genesis of the cerebral cortex and hippocampus (10, 11). The molecular mechanisms of these effects of choline have not been identified.

We reported that in the developing cerebral cortex, choline acts to modulate neural progenitor cell (NPC) self-renewal by regulating the synthesis of the full-length (isoform 1) epidermal growth factor receptor (EGFR), an essential component of a signaling pathway involved in

diverse cellular processes (11), including cortical neurogenesis (12–16). Yet, how choline controls EGFR synthesis remains unknown. In fetal brains from mouse dams fed a LC diet, we showed that *Egfr* mRNA was expressed normally, but the synthesis of the EGFR protein was inhibited (11). This result suggests that microRNAs (miRs; small noncoding RNAs) post-transcriptionally regulate the synthesis of the EGFR protein (17–19). However, whether miRs respond to nutrient status to modulate brain development has not been demonstrated.

In this study, we identified a specific miR, miR-129-5p, that is upregulated in LC NPCs, binds the 3′ UTR of *Egfr*, and inhibits its protein synthesis. Although expression of miR-129-5p was detected in the developing and adult brain, its role during neurogenesis has not been examined. In this study, miR-129-5p was up-regulated in cortical NPCs in response to LC status. We further found that inhibition of miR-129-5p function in the developing cortex *in vivo* is sufficient to restore NPC self-renewal in LC embryos. Together, our results demonstrate, for the first time to our knowledge, that NPC self-renewal and differentiation capacity in the developing cerebral cortex is controlled by choline availability through the regulation of miR expression. These findings provide a direct demonstration of a mechanism whereby metabolism of nutrients influences gene and protein expression during development.

MATERIALS AND METHODS

Animals

Mice were bred and maintained at the David H. Murdock Research Institute (DHMRI), Center for Laboratory Animal Science facilities. All experiments were performed in accordance with the standards of the U.S. National Institutes of Health (NIH) *Guide for Care and Use of Laboratory Animals* and were approved by the DHMRI Institutional Animal Care and Use Committee. *Nestin-CFPnuc* transgenic mice were generously provided by Dr. Grigori Enikolopov (Cold Spring Harbor Laboratory, Cold Spring Harbor, NY, USA) (20), and were maintained on a C57BL/6J background. The *Egfr^f* mouse line was kindly provided by Dr. David. W. Threadgill (Texas A&M University, College Station, TX, USA) (21). Genotyping for the *Nestin-CFPnuc* and *Egfr^f* lines was performed according to the providers' protocols (20, 21). *Nestin-CreER^{T2+/−}* and *Ai9* mouse lines were purchased from The Jackson Laboratory (Bar Harbor, ME, USA) and maintained on a C57BL/6J background (22, 23). Genotyping for *Nestin-CreER^{T2+/−}* and *Ai9* lines was performed according to protocols provided by The Jackson laboratory.

Diets

For at least 2 wk before mating, all animals were fed an AC diet (modified AIN93G diet with 1.4 g/kg choline chloride; D16040703Y; Research Diets, New Brunswick, NJ, USA) (Supplemental Fig. S4) through embryonic day (ED) 10. On ED 11, timed-pregnant mice were randomly assigned to 2 feeding groups: LC (LC; modified AIN93G diet with 0 g/kg choline chloride) or AC diet and were fed these diets until ED 17.

Neural progenitor cell culture

Neural progenitor cells were isolated from AC embryonic ED 14 brains and cultured as previously described (24). In brief, cerebral hemispheres from ED 14 embryos were dissected and dissociated into single cells. NPCs were grown in custom choline-free neurobasal medium, supplemented with 2 mM L-glutamine and B27 supplement without vitamin A (all from Thermo Fisher Scientific, Waltham, MA, USA). Choline chloride (MilliporeSigma, Burlington, MA, USA), dissolved in PBS and sterile filtered, was added to culture medium to final concentrations of 7 μM (LC) or 70 μM (AC) (25). For monolayer cultures, neurospheres were dissociated and plated in 24-well glass-bottom plates (MatTek, Ashland, MA, USA), precoated with polyornithine (MilliporeSigma) and fibronectin (MilliporeSigma). NPCs were incubated at 37°C, 5% CO_2.

S-adenosylmethionine treatment in cultured NPCs

Neural progenitor cells were cultured as previously described. *S*-adenosylmethionine (AdoMet), in the stable form of AdoMet-tosylate (Cayman Chemicals, Ann Arbor, MI, USA), was used at a final concentration in the medium of 100 μM.

Neural progenitor cell isolation for *in vivo* treatment experiments

For experiments in which diets/treatments were administered *in vivo*, nestinCFP⁺ cells were isolated by fluorescence-activated cell sorting (FACS) (Aria III sorter; BD Biosciences, Franklin Lakes, NJ, USA), from AC and LC ED 17 embryos. The isolated cell population was pelleted and stored at −80°C.

Transfection of neural progenitor cells

Neural progenitor cells were plated as monolayers for 24 h before transfection, as previously described. Transient transfections (DharmaFECT1 transfection reagent; Dharmacon, Lafayette, CO, USA) were conducted at 24 h of culture with miR-129-5p miRidian mimic and scrambled control miR (sc-miR) (Dharmacon). 5-Ethynyl-2′-deoxyuridine (EdU) was added to the culture medium at 10 μM for 24 h between 48 and 72 h of culture. EdU detection was performed at 72 h of culture with the Click-iT EdU Alexa Fluor 555 Detection Kit (Thermo Fisher Scientific), according to the manufacturer's protocol.

Genetic lineage tracing

Heterozygous *Egfr^{f/+}-Ai9^{+/−}* females (21) were mated to *Nestin-CreER^{T2+/−}* males (22, 23) to obtain *Egfr^{f/f}-Nestin-CreER^{T2+/−}-Ai9^{+/−}* and *Egfr^{+/+}-Nestin-CreER^{T2+/−}-Ai9^{+/−}* triple-transgenic littermates, and 1 mg tamoxifen (TM; MilliporeSigma) dissolved in 200 μl corn oil was administered to pregnant females at E12 by oral gavage. Embryos were collected at ED 17 for analysis.

In utero electroporation

Electroporation was performed, essentially as previously described (26, 27). In brief, 1–2 μl pooled plasmid DNA (1.5 μg/μl) and miRNAs were injected into the lateral ventricles of E14.5 brains with a Minj-D pressure injector (Tritech Research, Los Angeles, CA, USA) and electroporated by using five 50-ms pulses of 40 V and a 950-ms interpulse duration through the uterine wall using paddle electrodes and a NEPA21 electroporator (Nepagene, Ichikawa, Japan). Plasmids for electroporation were prepared by using the EndoFree Plasmid Maxi Kit (Qiagen, Hilden, Germany). The following DNA and miR combinations were used: pCAG-EGFP (plasmid 11150; Addgene, Cambridge, MA,

USA) control DNA and sc-miR (1 μg/μl) (Dharmacon); mixture of pCAG-EGFP and 40 picomoles of mature miR-129-5p (Dharmacon); mixture of locked nucleic acid–modified oligonucleotide miR-129-5p inhibitor (100 nM) (Exiqon; Qiagen) or sc-miR-inh, and pCAG-EGFP.

MiR microarrays

Cells were harvested from cultured NPCs for real-time PCR Taq-Man miRNA arrays. Total RNA was isolated from neural progenitor cells incubated in LC and AC medium by Qiazol miRNAeasy kits (Qiagen), according to the protocol described by the manufacturer. Reverse transcription was performed with Rodent MegaPlex RT Primer pools. cDNA was amplified by using rodent MegaPlex PreAmp Primer Pools and PreAmp Master mix (Thermo Fisher Scientific). The amplified samples were loaded into Taqman miR arrays (4470188; Thermo Fisher Scientific) and analyzed with the 7900 Real-Time PCR System (Thermo Fisher Scientific). C_t values were calculated by SDS 1.2 software (Thermo Fisher Scientific), normalized to MammU6 (miRNA) housekeeping C_t values, and expressed as $2^{-[Ct(miR) - Ct(U6)]}$.

RT-PCR analysis

Total RNA was isolated from cyan fluorescent protein (CFP)+AC and LC E17 NPCs isolated by fluorescence-activated cell sorting (FACS) with the miRNeasy mini kit (Qiagen). For each sample, cortices were pooled from 6 to 8 embryos in the litter. Mature miR-129-5p expression was quantified by real-time RT-PCR with a TaqMan miR assay kit for hsa-miR-129-5p (ID 00590; Thermo Fisher Scientific). Mouse U6 snRNA was used as internal control (ID 001973; Thermo Fisher Scientific). Real-time RT-PCR for primary precursor of miR-129-5p (pri-miR-129-5p, ID Mm03306410) was performed with RT^2 Sybr Green Quantitative PCR Master Mix (Thermo Fisher Scientific), with U6 used as the normalization control. For *Egfr* expression, primers were from Qiagen (ID PPM0714F) and TATA box binding protein was used as the normalization control. Values were normalized with the ΔC_t method as previously described.

Luciferase reporter assay

Human embryonic kidney (HEK 293T) cells were maintained in DMEM (Thermo Fisher Scientific), containing 10% FBS and 0.1 mM nonessential amino acids (Thermo Fisher Scientific), and seeded in a 96-well plate (2×10^4 cells/well) 24 h before transfection. Fifty nanomolar of the miR-129-5p miRidian mimic (Dharmacon) or scrambled control (sc-miR; Dharmacon) were cotransfected with 100 ng per well of the pEZXMT06 vector, containing the full-length 3′ UTR of *Egfr* (GeneCopoeia, Rockville, MD, USA), using Fugene HD (Promega, Madison, WI, USA), according to the manufacturer's protocol. To test binding specificity, EGFR 3′ UTR with mutations in the miR-129-5p recognition sites was subcloned into the pEZXMT06 vector and cotransfected with the control vector as previously described. Luciferase activity was measured 48 h after transfection with the Luc-Pair Luciferase assay kit (GeneCopoeia).

Site-directed mutagenesis

Site-directed mutagenesis (performed at GeneCopoeia) was conducted to change the GCAAAAA seed sequence in the 3′ UTR of *Egfr*. Two predicted miR-129-5p sites were mutated for CGUUU, to determine whether the putative site influenced

luciferase activity. Luciferase reporter assays were performed as previously described.

Western blot analysis

Cultured NPCs were used to evaluate EGFR levels. Protein extracts were prepared with RIPA lysis buffer supplemented with protease inhibitor cocktail (Roche, Basel, Switzerland). Total protein concentration for all samples was quantified by bicinchoninic assay (Bio-Rad, Hercules, CA, USA). Proteins were loaded into SDS-PAGE gels and blotted on PVDF membranes. Immunolabeling was accomplished with the following antibodies: EGFR (2232; Cell Signaling Technology, Danvers, MA, USA; this antibody is specific for the full-length isoform 1 and does not detect the truncated isoform 2) (28, 29), H3K23me3 (05-1951; MilliporeSigma), and total H3 (ab134198; Abcam, Cambridge, United Kingdom). The secondary antibodies were goat anti-rabbit horseradish peroxidase–conjugated, donkey anti-chicken 800CW (925-32218; Li-Cor Biosciences, Lincoln, NE, USA) and goat anti-mouse 600RD (925-68070; Li-Cor Biosciences). ECL (Thermo Fisher Scientific) was used to detect proteins. The membranes were imaged in a Li-Cor Odyssey imaging system.

AdoMet and *S*-adenosylhomocysteine assays

Embryonic brains from AC or LC mice were collected at E17, pulverized, and analyzed. Concentrations of AdoMet and *S*-adenosylhomocysteine (AdoHcy) were measured with an HPLC assay, as described by Molloy *et al.* (30).

Immunohistochemistry, microscopy, and data analysis

Embryonic brains were fixed in 4% paraformaldehyde and cryoprotected in a gradient of 10–30% sucrose/1× PBS solution. Coronal sections (20 μm) were prepared by cryosectioning. Brain sections were blocked with 0.1% Triton X-100 and 5% normal goat serum in 1× PBS for 1 h at room temperature. Incubation with primary antibodies was performed at 4°C overnight. Secondary antibodies were applied for 1 h at room temperature. Antibodies used and dilutions are as follows: rabbit polyclonal anti-EGFR detecting the intracellular EGFR domain (1:1000; Abcam), chicken polyclonal anti-EGFP detecting the intracellular EGFR domain (1:1000; Aves Labs, Togard, OR, USA), and rabbit monoclonal anti-Ki67 (1:500; Abcam). Antigen retrieval [10 nm sodium citrate (pH 6.0) in steam heat for 20 min] was performed for detection of Ki67. Secondary antibodies were goat anti-rabbit Cy3 (1:250; Jackson ImmunoResearch, West Grove, PA, USA), goat anti-chicken Alexa 488 (1:1000; Jackson ImmunoResearch). DAPI (1:2000; MilliporeSigma) was used to label nuclei. The Click-iT EdU kit (Thermo Fisher Scientific) was used to detect 5-ethynyl-2′-deoxyuridine incorporation (EdU; 10 μM; Click-iT Alexa Fluor 555 Kit; Thermo Fisher Scientific). Images were collected on a Zeiss LSM 710 confocal microscope (Zeiss GmbH, Oberkochen, Germany). Z-stacks were acquired for each coronal section with ×10, 20, or 40 objectives. Cell counts and tissue measurements were obtained with ImageJ (NIH; Bethesda, MD, USA) and LSM Browser (Zeiss GmbH) software.

Bioinformatics

MicroRNA target-prediction analysis was conducted with the miRanda (*http://www.microrna.org*) (31) and TargetScan (*http://genes.mit.edu/targetscan*) (32) algorithms.

Statistical analyses

The number of samples per group and the probabilities are indicated in the figure legends. Statistical analyses were performed with Prism 7 (GraphPad Software, La Jolla, CA, USA). Data distribution was tested for statistical normality. The Brown-Forsythe test (F test) was used to compare group variances. Groups with equal variances were compared using 1-Way ANOVA (more than 2 groups) or Student's t test (2 groups). Groups with unequal variances were compared using non-parametric Kruskal-Wallis (more than 2 groups) or Mann-Whitney (2 groups) tests. The χ^2 test was used to compare cell distribution in Fig. 4. Data are presented as means ± SEM.

RESULTS

MiR-129-5p is upregulated in LC NPCs and inhibits EGFR synthesis by binding its 3′ UTR

We previously found, *in vivo*, a substantial decrease in proliferating embryonic cortical NPCs (radial glia and intermediate progenitor cells), as well as a persistent decrease in the number of the upper-layer cortical neurons resulting from reduced choline availability during gestation (11). These changes in NPC properties were accompanied by a reduction in EGFR protein levels in embryonic cortical NPCs, which occurred because of aberrant EGFR protein synthesis, as opposed to changes in EGFR protein or mRNA stability. We therefore sought to examine whether lowering choline availability in the fetal brain would lead to upregulation of miRs that would in turn regulate the synthesis of EGFR.

To identify which miRs expressed in cortical NPCs may be sensitive to choline availability, we used *NestinCFPnuc*$^{+/-}$ transgenic animals, in which CFP marks predominantly radial glial cells (11). When expanded in culture, NPCs isolated from *NestinCFPnuc*$^{+/-}$ express nestin, suggesting that they maintain the properties of radial glia *in vitro*. We previously demonstrated that, in this culture model, low levels of choline induce changes in NPC self-renewal, mimicking the behavior of LC CFP-expressing NPCs *in vivo* (11). We first screened for changes in miR expression in primary NPCs cultured for 48 h in response to LC (7 μM) *vs.* AC (70 μM) levels. Using real-time PCR-based miR arrays, we detected statistically significant changes in the expression of 11 miRs between AC and LC NPCs (**Fig. 1A**), suggesting that an LC maternal diet does not induce major defects in miR-processing machinery, but specifically affects the expression of select miRs.

We reasoned that reduction of EGFR protein in NPCs could be mediated by miRs that were up-regulated in LC conditions, both *in vitro* and *in vivo*, and could target full-length *Egfr* 3′ UTR. Using the TargetScan algorithm (www.targetscan.org) (32), we determined that, among the miRs up-regulated in LC NPCs, miR-129-5p is predicted to target the full-length *Egfr* 3′ UTR at the 4 binding sites that are conserved between the mouse and the human (Fig. 1G). We next used qPCR to confirm that miR-129-5p up-regulation under LC conditions would also be observed *in vivo*. We found a more than 2-fold increase in miR-129-5p expression in LC CFP-expressing NPCs isolated from

Nestin-CFP$^{+/-}$ cortices by FACS (Fig. 1B). Furthermore, up-regulation of miR-129-5p occurred at the transcriptional level; expression of the primary precursor of miR-129-5p in FACS-identified LC NPCs was ~5-fold higher than in AC NPCs (Fig. 1C).

To test whether miR-129-5p functions to regulate EGFR synthesis in NPCs, we transfected AC NPCs with miR-129 mimics (Fig. 1D, E). No changes in *Egfr* mRNA expression were detected among the groups (Fig. 1D). However, we found that miR-129-5p–transfected NPCs had a significant reduction in EGFR protein levels (Fig. 1E, F). These data demonstrate that miR-129-5p targets *Egfr* and inhibits its protein synthesis in NPCs. To confirm that miR-129-5p targets *Egfr* through its predicted binding sites, we transfected HEK293T cells with a firefly/*Renilla* dual-luciferase reporter vector, pEZX-MT06, containing the full-length mouse *Egfr* 3′ UTR, along with mature miR-129-5p. An ~50% reduction of the reporter luciferase activity was observed when cells were transfected with miR-129-5p (Fig. 1H). To demonstrate that this repression is caused by the specific binding of miR-129-5p to *Egfr* 3′ UTR, we introduced mutations in miR-129-5p binding sites within the *Egfr* 3′ UTR. Mutations in the *Egfr* 3′ UTR abolished reporter repression by miR-129-5p (Fig. 1I). Consistent with the reduction in EGFR protein levels, miR-129-5p alters NPCs proliferative capacity, evidenced by the reduced incorporation of EdU in transfected miR-129-5p compared with AC NPCs (Fig. 1J–L). Together, these results demonstrate that LC availability results in the up-regulation of miR-129-5p expression in NPCs, which inhibits EGFR protein synthesis, thus altering NPC proliferative and differentiation capacity.

Egfr haploinsufficiency in NPCs, as well as LC availability, disrupt cortical neurogenesis *in vivo*

We reasoned that if EGFR protein levels were regulated by choline *via* miR-129-5p *in vivo*, we could expect loss of EGFR function to replicate the neurogenesis defects caused by the reduction in choline supply. To examine whether reduction in EGFR protein levels in NPCs disrupts neurogenesis, we generated triple-transgenic *Egfr*$^{f/+}$-*Nestin-CreER*$^{T2+/-}$-*Ai9*$^{+/-}$ embryos, in which activation of Cre recombinase and deletion of 1 copy of *Egfr* in nestin-expressing NPCs can be achieved in a temporally controlled manner by administration of TM (**Fig. 2A**) (21–23). Cells in which Cre was activated, and all their progeny, were permanently labeled by the expression of tdTomato fluorescent protein from the *Ai9* Cre-reporter allele. Based on our observations that EGFR protein levels are reduced in LC NPCs *in vivo* as early as E14 (11), we treated pregnant females with TM at E12 to allow sufficient time for TM-induced recombination to occur. We first confirmed that TM-induced inactivation of 1 copy of *Egfr* allele in *Egfr*$^{f/+}$-*Nestin-CreER*$^{T2+/-}$-*Ai9*$^{+/-}$ embryos results in the reduction in EGFR protein levels in cortical NPCs. Using immunostaining, we found that tdTomato-expressing cells in *Egfr*$^{f/+}$-*Nestin-CreER*$^{T2+/-}$-*Ai9*$^{+/-}$ E17 embryos contained reduced amounts of EGFR protein
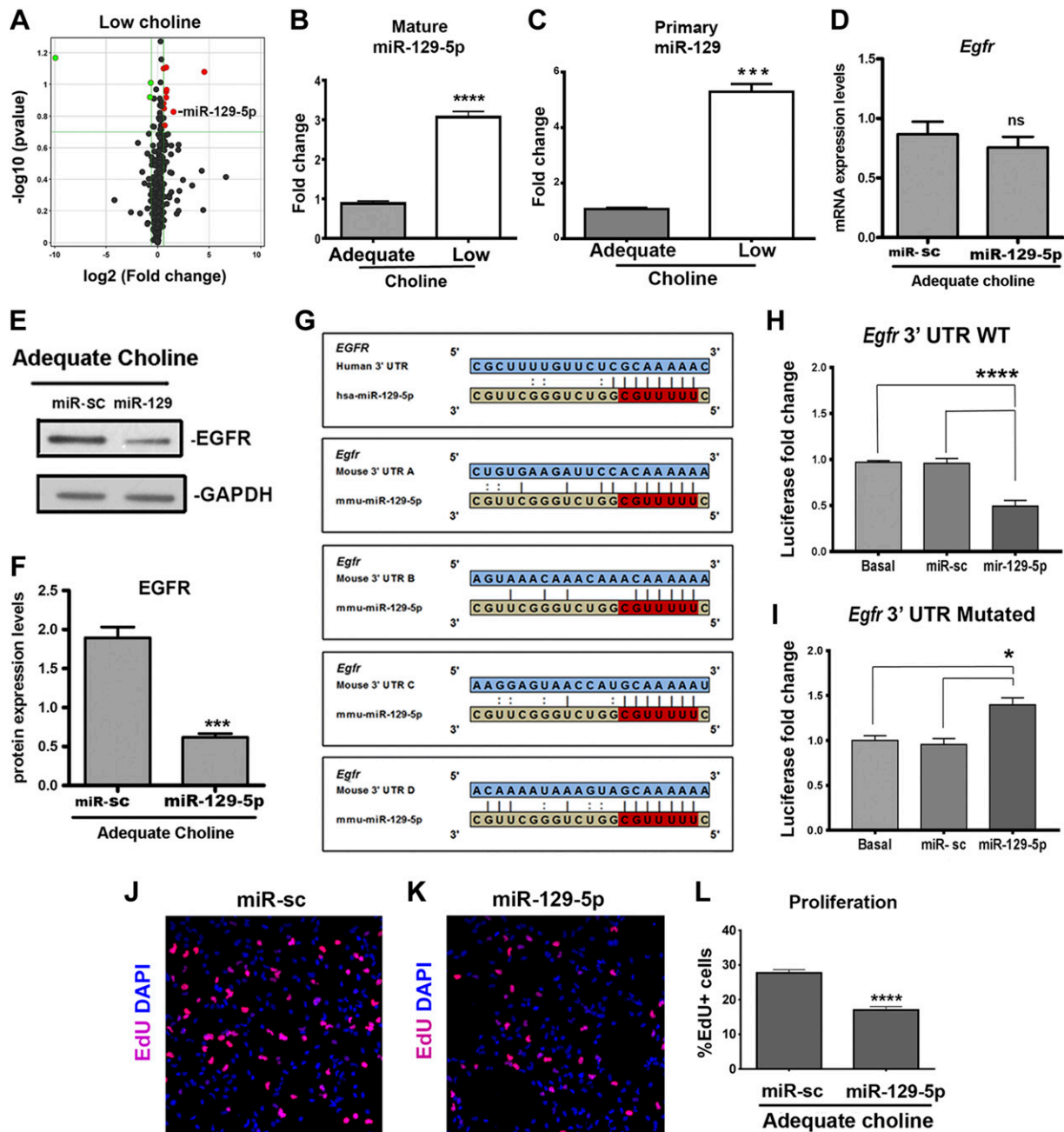
Figure 1. MiR-129-5p is upregulated in NPCs in response to LC availability, binds *Egfr* 3′ UTR and regulates EGFR protein synthesis. *A*) Cortical NPCs were cultured in LC (7 μM)- or AC (70 μM)-containing medium for 48 h, and real-time PCR-based miRNA arrays were used to detect changes in miRNA expression between the samples. Values are a volcano plot of significant and differential LC-associated miRNA changes (change >1.5-fold; $P < 0.2$), with increased expression shown in red and decreased expression in green. *B*) Levels of mature miR-129-5p were quantified by real-time PCR with individual miR assays in nestinCFP-expressing cells isolated from LC and AC embryonic day (ED) 17 cortices by FACS. Relative quantitative values (normalized to U6 snRNA) are reported as fold change ($n = 5$ per group). Data are means ± SEM. ****$P < 0.0001$, by Student's *t* test. *C*) Expression levels of primary miR-129-5p transcript were quantified by real-time PCR in nestinCFP-positive LC and AC ED 17 NPCs isolated by FACS. Relative quantitative values (normalized to U6) are reported as fold change ($n = 6$ per group). Data are means ± SEM. ***$P = 0.001$, by Mann-Whitney test. *D*) Cultured cortical NPCs were transfected with sc-miR or miR-129-5p mimics and cultured for 48 h. No changes in *Egfr* mRNA expression between conditions were detected by real-time PCR ($n = 4$ per group). *E, F*) Cultured cortical NPCs were transfected with sc-miR or miR-129-5p mimics and were cultured in AC (70 μM) medium for 48 h. *F*) EGFR protein levels normalized to GAPDH protein levels, examined by Western blot ($n = 4$ per group), were reduced in NPCs transfected with miR-129-5p mimics compared to sc-miR. Data are means ± SEM. ***$P < 0.001$, by Student's *t* test. *G*) miR-129-5p binding sites within *Egfr* 3′ UTR in red. *H*) HEK 293T cells were cotransfected with firefly/*Renilla* dual-luciferase reporter vector, pEZX-MT06, containing the full-length mouse *Egfr* 3′ UTR, and sc-miR or mature miR-129-5p. Reduction in luciferase activity was detected in miR-129-5p-transfected cells ($n = 8$ per group). ****$P < 0.0001$, by 1-way ANOVA. *I*) Cotransfection of the luciferase reporter vector carrying mutated *Egfr* 3′ UTR and mature miR-129-5p did not reduce luciferase activity in HEK293T cells. *$P < 0.05$, by 1-way ANOVA. *J–L*) NPCs were cultured in AC conditions for 24 h, transfected with sc-miR (*J*) or miR-129-5p (*K*) mimics and cultured for another 48 h. EdU was added for 24 h at 48 h of culture. Misexpression of miR-129-5p mimics reduces the proportion (*L*) of EdU⁺ cells (red) among all NPCs ($n = 8$ per group). ****$P < 0.0001$, by Mann-Whitney test.
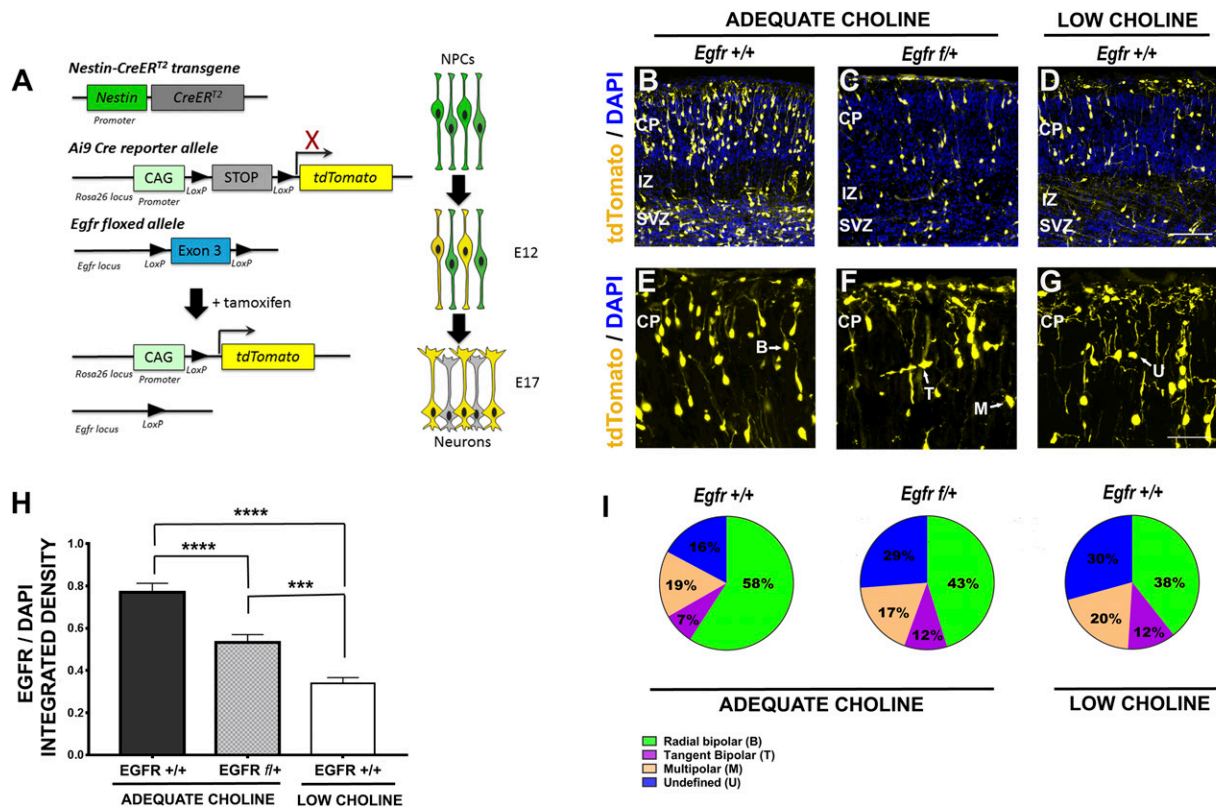
Figure 2. *Egfr* haploinsufficiency in *Egfr* $^{f/+}$-*Nestin-CreER*$^{T2+/−}$-*Ai9*$^{+/−}$ cortical NPCs, as well as LC availability during gestation, disrupt cortical neurogenesis in embryonic day (ED) 17 embryos. *A*) TM-induced recombination in the *Ai9* allele, leading to expression of tdTomato in NPCs and their progeny and deletion of the floxed 3d exon of *Egfr* (*Egfr* $^{f/+}$). *B*) Expression of tdTomato, induced in AC *Egfr*$^{+/+}$-*Nestin-CreER*$^{T2+/−}$-*Ai9*$^{+/−}$ embryos at ED 12 and analyzed at ED 17, demonstrated mosaic labeling of cells within the VZ/SVZ and pyramidal neurons migrating to the CP; the IZ is also shown. *C*) Compared to AC *Egfr*$^{+/+}$-*Nestin-CreER*$^{T2+/−}$-*Ai9*$^{+/−}$ littermates, tdTomato-labeled cells in AC *Egfr* $^{f/+}$-*Nestin-CreER*$^{T2+/−}$-*Ai9*$^{+/−}$ cortices are reduced in number in the VZ/SVZ and the CP. *D*) Fewer tdTomato cells in the VZ/SVZ and the CP are also observed in the cortices of LC ED 17 embryos when tdTomato expression is induced at ED 12. *E*) Most of the labeled pyramidal neurons in the CP of AC *Egfr*$^{f/+}$-*Nestin-CreER*$^{T2+/−}$-*Ai9*$^{+/−}$ embryos exhibit bipolar morphology, with clearly defined processes. *F*) Pyramidal neurons in the CP of *Egfr*$^{f/+}$-*Nestin-CreER*$^{T2+/−}$-*Ai9*$^{+/−}$ embryos appear disorganized, with some cells exhibiting multiple processes. *G*) Neurons in the CP of LC ED 17 embryos, in which tdTomato expression was activated at ED 12, also exhibit abnormal morphology, with many neurons appearing multipolar and round (undefined). *H*) Quantification of EGFR protein levels was performed in control *Egfr*$^{+/+}$-*Nestin-CreER*^{T2}-*Ai9*$^{+/−}$ and *Egfr*$^{+/−}$-*Nestin-CreER*^{T2}-*Ai9*$^{+/−}$ tdTomato-expressing NPCs by detection of immunofluorescence (n = 4–6 embryos per group). ***$P < 0.001$ by Student's *t* test. *I*) Venn diagrams depicting distribution of labeled neurons in the CP of AC *Egfr*$^{+/+}$-*Nestin-CreER*$^{T2+/−}$-*Ai9*$^{+/−}$, *Egfr* $^{f/+}$-*Nestin-CreER*$^{T2+/−}$-*Ai9*$^{+/−}$ and LC ED 17 embryos demonstrate reduction in the proportions of cells with bipolar morphology (green) and increase in cells with undefined morphology (blue) in *Egfr* $^{f/+}$-*Nestin-CreER*$^{T2+/−}$-*Ai9*$^{+/−}$ and LC embryos compared to AC embryos. ***$P < 0.001$, ****$P < 0.0001$, by 1-way ANOVA. B, bipolar; M, multipolar; T, migrating tangentially; U, undefined. Scale bars: 100 μm (*D*); (*G*): 60 μm.

(Fig. 2*H* and Supplemental Fig. S1*A*). Moreover, compared to control *Egfr*$^{+/+}$-*Nestin-CreER*$^{T2+/−}$-*Ai9*$^{+/−}$ embryos, 1 dose of TM at E12 consistently resulted in fewer tdTomato-labeled cells in the E17 cortices of *Egfr*$^{f/+}$-*Nestin-CreER*$^{T2+/−}$-*Ai9*$^{+/−}$ embryos (Fig. 2*B, E vs.* Fig. 2*C, F*). In contrast to migrating and differentiating neurons in control *Egfr*$^{+/+}$-*Nestin-CreER*$^{T2+/−}$-*Ai9*$^{+/−}$ brains, most of which were elongated with distinct bipolar morphology (Fig. 2*E*), the proportions of tdTomato-expressing cells in the cortical plate (CP) of *Egfr*$^{f/+}$-*Nestin-CreER*$^{T2+/−}$-*Ai9*$^{+/−}$ brains that clearly exhibit bipolar morphology in apicobasal orientation are significantly reduced, the proportions of tangentially migrating cells, as well as cells with undefined morphology increased, whereas the proportions of multipolar cells remained unchanged (Fig. 2*B, E vs.* Fig. 2*C, F*; Fig. 2*I* and Supplemental Table S1).

To further confirm that reduction in EGFR protein levels leads to defects in neurogenesis similar to those caused by LC, we induced activation of Cre recombinase in *Nestin-CreER*$^{T2+/−}$-*Ai9*$^{+/−}$ embryos derived from dams fed an LC diet between ED 11 and ED 17, and characterized tdTomato-labeled cells in the CP at ED 17. We found that, similar to *Egfr*$^{f/+}$-*Nestin-CreER*$^{T2+/−}$-*Ai9*$^{+/−}$ brains, the number of tdTomato-labeled cells was consistently reduced in LC brains, whereas the proportions of labeled cells with elongated bipolar morphology were also significantly decreased, whereas the proportions of undefined cells increased in LC *vs.* AC *Egfr*$^{+/+}$-*Nestin-CreER*$^{T2+/−}$-*Ai9*$^{+/−}$ E17 cortices (Fig. 2*B, E vs.* Fig. 2*D, G*; Fig. 2*I* and Supplemental Table S1). These results show that partial loss of EGFR function in NPCs reduces the proportion of radially migrating differentiating neurons

and increases the proportions of cells with abnormal morphology in the cortical wall, similar to the effects induced by LC availability.

Inhibition of miR-129-5p function in LC cortical NPCs is sufficient to restore neurogenesis

To examine whether inhibiting miR-129-5p function in LC NPCs would restore their self-renewal capacity, we first evaluated incorporation of EdU in NPCs cultured in adequate or LC conditions. NPCs were transfected with either control locked nucleic acid–modified oligonucleotide scrambled inhibitor or miR-129-5p inhibitor (**Fig. 3***A–D*). Consistent with our predictions, inhibiting miR-129-5p function in LC NPCs restores the proportion of EdU$^+$ cells among the transfected NPCs (Fig. 3), confirming our hypothesis that miR-129-5p mediates the effect of LC on NPC self-renewal.

Next, we sought to determine whether inhibiting miR-129-5p in the developing LC cortex *in vivo* would restore the genesis of cortical neurons. An miR-129-5p inhibitor or an sc-miR-inh, along with pCAG-EGFP DNA plasmid, was introduced into E14 cortical NPCs by *in utero* electroporation. We found that EGFR expression levels were

Figure 3. Inhibition of miR-129-5p function restores NPC self-renewal and EGFR protein levels in LC NPCs. *A–C*) NPCs were cultured for 24 h in AC (70 μM) medium, transfected with control sc-miR-inh (*B*) or miR-129-5p (*C*) inhibitor (miR-129-Inh), along with pCAG-EGFP plasmid, and further cultured in AC (70 μM) (*A*) or LC (7 μM) conditions for another 48 h. EdU was added for 1 h at the end of the culture period. Transfection of miR-129-inh restores the proportion of proliferating EdU$^+$ cells in LC conditions (*C*), compared to LC NPCs transfected with sc-miR-inh (*B vs. C*). *D*) Quantification of EdU$^+$ cells among transfected NPCs (*n* = 4 per group). *P < 0.05, ***P < 0.001 by 1-way ANOVA. *E*) Quantification of EGFR protein levels was performed in EGFP-expressing cells coelectroporated with miR-129-inh *vs.* sc-miR-inh in LC E17 cortices by detection of immunofluorescence. **P < 0.01, by Mann-Whitney test.

increased in EGFP-expressing NPCs transfected with miR-129-5p inhibitor *in vivo* (Fig. 3*E*).

Consistent with our previous finding that NPC self-renewal and the production of pyramidal neurons are substantially reduced because of LC supply, we observed fewer EGFP-expressing cells transfected with sc-miR in the CP of LC embryos at E17, as compared to brains from embryos exposed to AC (**Fig. 4***A vs.* Fig. 4*B*). Inhibiting miR-129-5p in LC NPCs restored the density of EGFP-labeled cells in the CP of LC E17 embryos (Fig. 4*C vs.* Fig. 4*B*). Furthermore, most of the EGFP-expressing cells in the ventricular and subventricular zones (VZ and SVZ) of LC cortices lacked expression of Ki67, a proliferative cell marker (Fig. 4*E vs.* Fig. 4*D*), suggesting that they had exited the cell cycle, whereas EGFP-expressing NPCs transfected with miR-129-5p inhibitor in LC cortices coexpressed Ki67 (Fig. 4*F vs.* Fig. 4*E*), suggesting that their self-renewal properties are restored. Consistent with our previous observations (see Fig. 2) (11), many EGFP-expressing cells in the CP of LC embryos exhibit small cell body size and do not possess characteristic bipolar morphology observed in AC cortices (Fig. 4*H vs.* Fig. 4*G*, arrowheads). On the contrary, when miR-129-5p inhibitor is introduced into cortical NPCs of LC embryos, differentiating neurons exhibiting typical bipolar morphology are observed among EGFP-expressing cells (Fig. 4*I vs.* Fig. 4*H*, arrowheads). The distribution of EGFP-labeled cells in the CP of LC embryos transfected with sc-miR-inh, showing reduced proportions of cells observed at midlevels of the cortical wall [SVZ and intermediate zone (IZ)], suggest that newly born, migrating neurons are reduced in LC brains (Fig. 4*K, L*; also see Supplemental Fig. S1*B*). Expression of miR-129-5p inhibitor in LC NPCs partially restores the distribution of EGFP-labeled cells in the cortical wall, with larger proportions of EGFP-expressing cells now observed in the IZ compared with LC cortices transfected with sc-miR-inh (Fig. 4*K*; also see Supplemental Fig. S1*B*). In contrast, when miR-129-5p is misexpressed in cortical NPCs, EGFP-labeled cells localize primarily to the IZ (Supplemental Fig. S2), suggesting that sustained maintenance of miR-129-5p expression in differentiating neurons prevents their proper placement in the cortical wall. These data demonstrate that inhibition of miR-129-5p function in LC NPCs restores their self-renewal and differentiation capacity, evidenced by an increase in EGFP-labeled cells expressing proliferative marker Ki67 in the VZ, and an increase in migration of cells located in the SVZ/IZ into the CP.
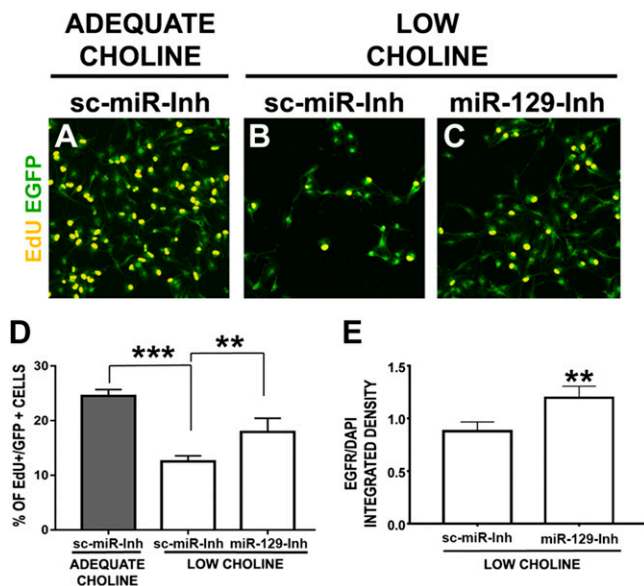
Choline-mediated changes in methylation potential regulate expression of miR-129-5p in NPCs

One of the important functions of choline is to serve as a methyl-group donor used for the synthesis of Ado-Met (1). AdoMet concentrations are diminished, and *S*-adenosylhomocysteine (AdoHcy) concentrations are increased in animals consuming LC diets (33, 34); the ratio of these 2 metabolites determines the rate of methylation reactions (35, 36). Therefore, we assayed AdoMet and AdoHcy concentrations in AC and LC E17 brains. We find that AdoMet concentrations and the AdoMet:AdoHcy
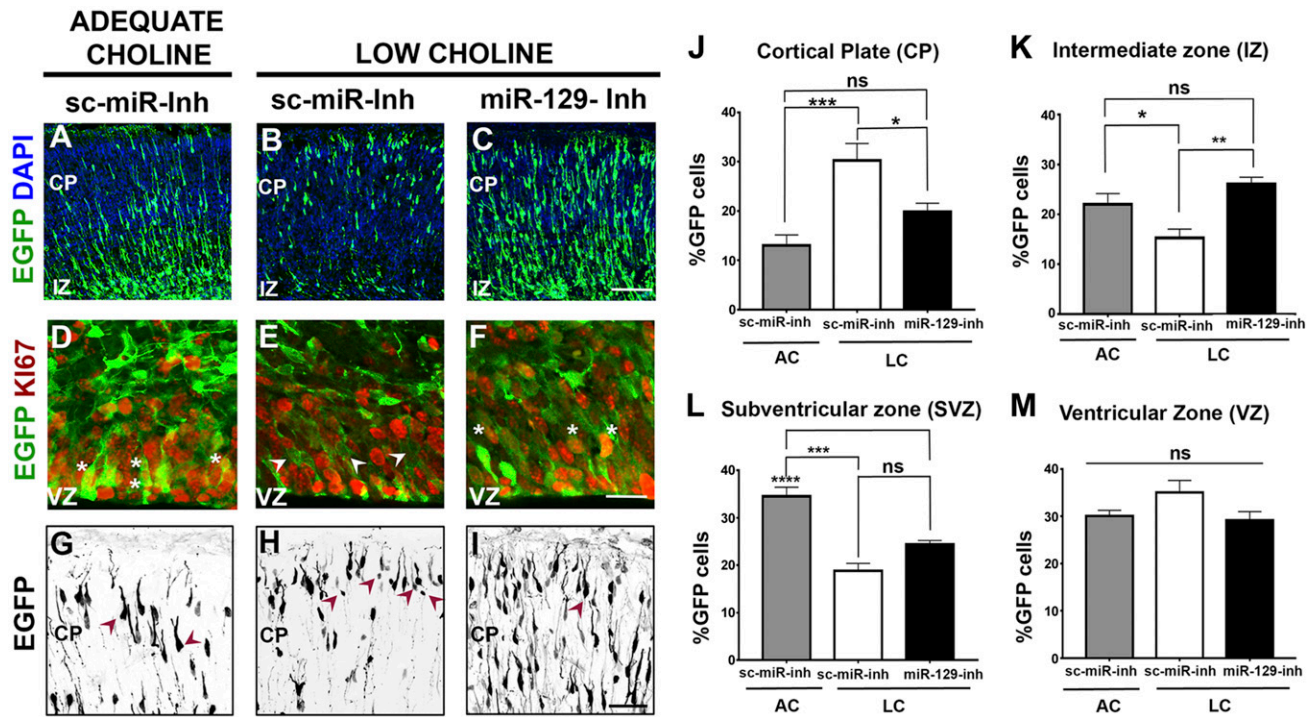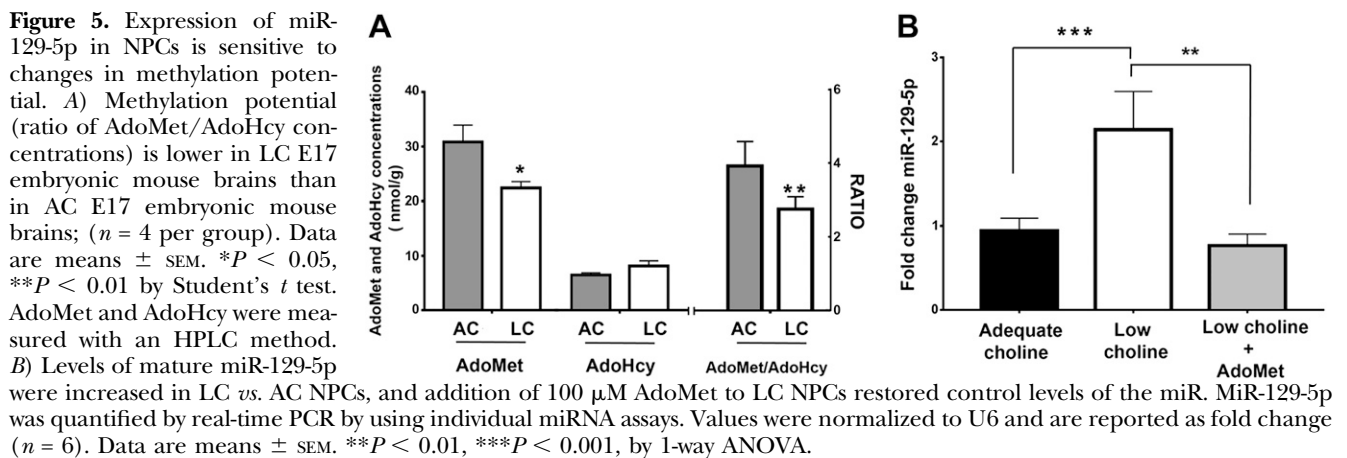
Figure 4. Inhibition of miR-129-5p function in NPCs restores neurogenesis in the LC E17 cortex. *A*) In AC embryos transfected with sc-miR-inh, EGFP-labeled cells were found in the VZ and SVZ and migrating toward the CP. *B*) EGFP-labeled cells in LC cortex were consistently fewer in number *vs.* the AC cortex and were primarily located in the VZ and the CP. *C*) Electroporation of LC cortex with miR-129-5p inhibitor restored the distribution of EGFP-labeled cells across the different layers of the cerebral wall and increased their number. *D–F*) Expression of EGFP and the proliferative cell marker Ki67 in the VZ/SVZ of transfected embryonic cortices. EGFP (*D*) was coexpressed with Ki67 in cells electroporated with sc-miR-inh (asterisks). VZ of LC embryos (*E*) contained many EGFP$^+$ cells that did not express Ki67 (arrowheads). Most EGFP$^+$ cells (*F*) electroporated with miR-129-inh in LC embryos expressed Ki67 (asterisks). *G*) AC pyramidal neurons transfected with sc-miR-inh exhibit typical morphology of immature pyramidal neurons (arrowheads). *H*) EGFP-expressing cells in the CP of LC embryos displayed a small cell body size and abnormal morphology (arrowheads). *I*) Transfection of LC NPCs with miR-129-5p inhibitor improves differentiating pyramidal cell morphology (arrowhead). *J–M*) Comparison of proportions of EGFP-expressing cells in the cortical walls of LC embryos transfected with sc-miR-inh and LC embryos transfected with miR-129-inh (*n* = 4 per group) demonstrated increased proportions of labeled cells in the CP (*J*) and reduced proportions of cells located in the IZ (*K*) and the SVZ (*L*), compared with AC embryos transfected with sc-miR-inh. Inhibition of miR-129-5p function in LC cortices decreased the proportion of cells occupying the CP (*J*) and increased the proportions of cells occupying the IZ (*K*). *P < 0.05, **P < 0.01, ***P < 0.001, ****P < 0.0001 by 1-way ANOVA test. At least 3 embryos per condition were analyzed. Scale bars: 100 μm(*C*); 35 μm (*F*); 50 μm (*I*).

ratio were significantly diminished in LC embryonic brains (**Fig. 5***A*). To investigate whether increasing AdoMet availability can restore miR-129-5p expression in LC NPCs, we examined the expression of mature miR-129-5p in LC NPCs treated with AdoMet. We found that the addition of

exogenous AdoMet to LC cultured NPCs reduced miR-129-5p expression levels (Fig. 5*B*).

Choline is a potent modifier of epigenetic marks (33), and we asked whether epigenetic marks previously reported to regulate miR-129-5p expression in cancer cells

Figure 5. Expression of miR-129-5p in NPCs is sensitive to changes in methylation potential. *A*) Methylation potential (ratio of AdoMet/AdoHcy concentrations) is lower in LC E17 embryonic mouse brains than in AC E17 embryonic mouse brains; (*n* = 4 per group). Data are means ± SEM. *P < 0.05, **P < 0.01 by Student's *t* test. AdoMet and AdoHcy were measured with an HPLC method. *B*) Levels of mature miR-129-5p were increased in LC *vs.* AC NPCs, and addition of 100 μM AdoMet to LC NPCs restored control levels of the miR. MiR-129-5p was quantified by real-time PCR by using individual miRNA assays. Values were normalized to U6 and are reported as fold change (*n* = 6). Data are means ± SEM. **P < 0.01, ***P < 0.001, by 1-way ANOVA.

are changed by choline availability in NPCs. Luan *et al.* (37) previously reported that miR-129-5p expression is modulated by a promoter histone 3 modification (H3K27me3). We did not find choline-induced alterations in global H3K27me3 in NPCs (Supplemental Fig. S3*A, B*). In gastric cancer cells, expression of miR-129-5p is controlled by DNA methylation at a specific CpG island located upstream of miR-129-5p transcriptional start site (38). However, we detected no changes in the methylation status of this CpG island in cultured cortical NPCs in response to choline availability (Supplemental Fig. S3*C*). Thus, we concluded that the 2 known epigenetic marks that regulate miR-129-5p expression are not differentially methylated in brain NPCs.

Based on our findings, we propose a model whereby LC availability during gestation lowers methylation potential in the developing brain, leading to up-regulation of miR-129-5p expression in cortical NPCs (**Fig. 6**). As a consequence, synthesis of full-length EGFR protein is inhibited by miR-129-5p, disrupting NPC self-renewal capacity and production of pyramidal neurons in the developing cerebral cortex.

DISCUSSION

For the first time to our knowledge, we have identified the molecular links that explain how a change in the availability of the dietary nutrient choline can modify important developmental processes in the brain. Specifically, we demonstrate that, in LC conditions, methylation potential (the AdoMet:AdoHcy ratio) is reduced in embryonic mouse brains and that this effect is associated with increased expression of miR-129-5p, whose role in the developing brain has not been examined. When miR-129-5p expression in NPCs increases, the synthesis of EGFR is blocked, disrupting neurogenesis.

The role of miR-129-5p in the regulation of brain development, or as an effector of nutrient status, has not been reported. Expression of miR-129-5p is enriched in the developing brain, and in neurons, specifically (39–41), where its known targets are fragile X mental retardation 1 and voltage-gated potassium channel Kv1.1 (42), suggesting an important role for miR-129-5p in the maintenance of neuronal function and homeostasis. In the proliferating progenitor cells of the developing retina (RPCs), however, miR-129-5p is known to inhibit the synthesis of transcription factors necessary for the acquisition of RPC competence to generate late born retinal cell types (43). The capacity of miR-129-5p to block cell cycle progression, in a manner similar to what we observed in NPCs (Figs. 1, 3, and 4), is consistent with its role in inhibiting cycle-dependent kinase 6 in lung cancer cells, as well as its role in inhibiting the growth of hepatocellular carcinoma cells through targeting p21-activated kinase 5 (44). Thus, the diverse functions of miR-129-5p and the selection of its targets appear to depend on the cellular context. Further investigation into whether miR-129-5p expression is modulated by nutrient status in tissues other than the developing brain is necessary. In addition to regulating mRNA stability (45), miR-129-5p is reported to function
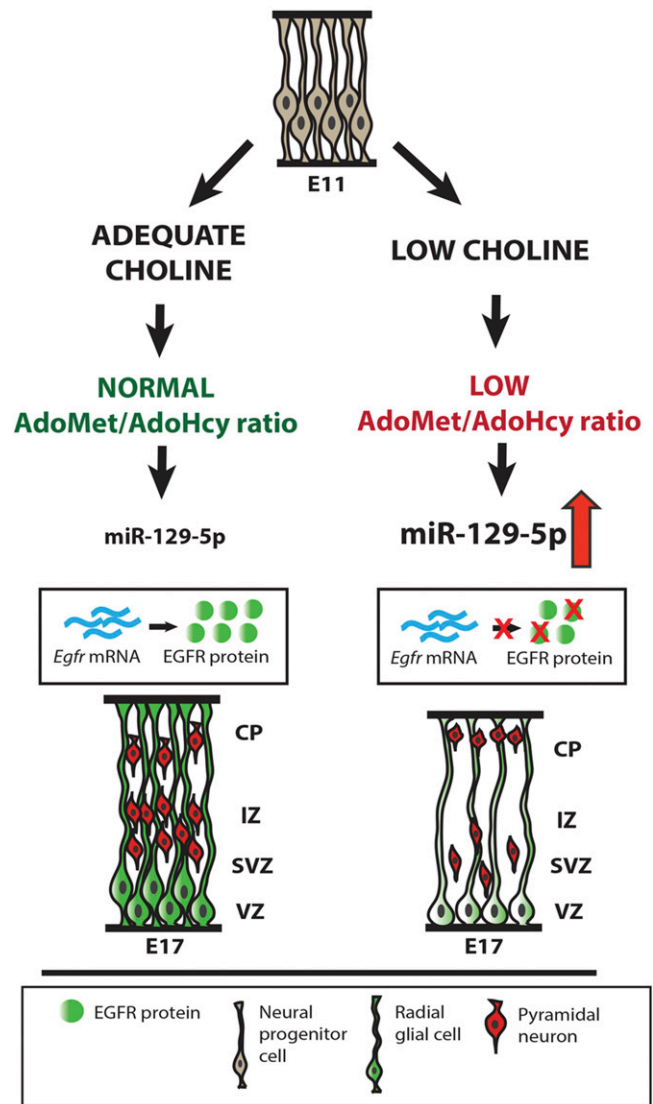

Figure 6. The effects of an LC maternal diet on cortical neurogenesis. LC maternal diet between E11 and E17 leads to a reduction in the methylation potential (AdoMet:AdoHcy ratio) in the developing brain. Reduced methylation potential is accompanied by upregulation of miR-129-5p and downregulation of its target, EGFR protein, in cortical NPCs (radial glia). Reduced levels of EGFR, in turn, alter NPC self-renewal capacity, resulting in the reduction in the number of NPCs, as well as cortical pyramidal neurons migrating toward the upper layers of the CP.

through inhibiting protein synthesis of its select known targets (42–44, 46), consistent with our findings that it is involved in post-transcriptional regulation of EGFR synthesis downstream of choline.

To date, the role of EGFR loss of function in the developing brain *in vivo* has been characterized primarily on a gross-morphologic level or in culture. Frontal brain regions, such as prefrontal cortex and olfactory bulbs, degenerate in *Egfr* congenic knockout and brain-specific knockout animals shortly after birth, whereas EGF-dependent proliferation of NPCs *in vitro* is diminished by the loss of *Egfr* (47–50). Similarly, loss of EGFR function in the developing retina leads to premature depletion of mitotic RPCs (51). In contrast, EGFR gain of function in

cortical NPCs, as well as in RPCs, promotes neuronal migration and acquisition of glial cell fate (12, 13, 52). We extended these findings by demonstrating that partial loss of EGFR function in cortical NPCs *in vivo* results in aberrant neurogenesis. Specifically, NPC self-renewal and generation of radially migrating cortical neurons in $Egfr^{f/+}$-$Nestin$-$CreER^{T2+/-}$-$Ai9^{+/-}$ embryos were compromised, whereas the proportions of tangentially migrating cells and cells with aberrant, round morphology, increased (Fig. 2*l*). Although we detected discrepancies between the effects of partial loss of EGFR function in NPCs *vs.* low availability of choline in the maternal diet on the proportions of radially and tangentially migrating cells and cells with aberrant, undefined morphology, these may be attributable to possible differential requirements for choline and EGFR signaling in migrating neurons, as well as in cortical NPCs *vs.* NPCs giving rise to interneurons. Expression levels of known EGFR ligands do not change in LC brains, whereas increasing concentrations of these ligands do not restore LC NPC self-renewal, suggesting that the receptor itself is the limiting factor in LC-induced defects in cortical neurogenesis (11).

Two isoforms of *Egfr* are present in the mouse: full-length isoform 1, and a truncated isoform 2, which lacks an intracellular tyrosine kinase domain (53). In this study, we found 4 miR-129-5p binding sites in a 3′ UTR specific to the full-length isoform 1 of *Egfr* (Fig. 1). In addition, down-regulation of EGFR protein induced by LC availability to NPCs disrupts the EGFR downstream signaling cascade (11), which relies on a functional tyrosine kinase domain. Moreover, we previously demonstrated that an miR-resistant form of full-length EGFR, EGFR-EGFP fusion protein lacking *Egfr* isoform 1 3′ UTR, is sufficient to restore the self-renewal capacity of LC NPCs (11), further supporting our conclusions that low availability of choline leads to post-transcriptional inhibition of EGFR synthesis through its 3′ UTR. Thus, our results represent the first evidence of sensitivity of EGFR protein synthesis to nutrient availability and to miR-129-5p-mediated inhibition, as well as the requirement for adequate EGFR protein levels to maintain cortical NPC self-renewal and differentiation capacity.

The long-term consequences of LC availability during pregnancy for neuronal differentiation and function remain unclear. We found that the morphologies of differentiating cortical pyramidal neurons are abnormal under LC conditions (Fig. 4). Low choline intake during pregnancy is associated with lower scores on visual memory tests in children (8). Studies addressing the role of choline in neuronal maturation and physiology are needed to understand how cognitive function may be affected by choline supply during development.

Finally, we showed that restoring AdoMet and methylation potential in NPCs prevents choline-mediated increase in miR-129-5p expression (Fig. 5). This finding strongly suggests that the effects of choline in NPCs are mediated through its role as a methyl donor and not *via* its role in phospholipid synthesis. Loss of histone methylation because of reduced methylation potential caused by LC availability is a plausible mechanism whereby expression of miR-129-5p could be increased in LC NPCs. In

breast cancer cells, expression of mir-129-5p is regulated through the establishment of histone marks. Specifically, enhancer of zeste homolog-2 mediates the trimethylation of lysine 27 on histone H3 (H3K27me3) in the promoter region of the miR-129-5p, leading to down-regulation of its expression (37). AdoMet levels constitute a limiting factor affecting the extent of histone methylation (54). However, we did not find methylation changes in global H3K27me3 in NPCs with LC availability (Supplemental Fig. S3). Loss of DNA methylation is also a plausible mechanism whereby expression of miR-129-5p could be increased in LC NPCs. Such a mechanism was reported for the regulation of miR-129-5p expression in gastric cancer cell lines (38). However, we found that methylation changes in the CpG islands reported to control miR-129-5p expression in cancer cells were not observed in LC NPCs. Methyltransferases are essential in epigenetic control, lipid biosynthesis, protein repair, hormone inactivation, and tissue differentiation; there are at least 208 proteins in the human genome that are identified as known or putative methyltransferases (55). More research is needed to identify which of these methyltransferases mediates the effects of choline-mediated changes in methylation potential on miR-129-5p expression.

Our results demonstrate that in response to the low availability of choline and because of the accompanying reduction in the methylation potential in the developing brain, miR-129-5p expression is increased in cortical NPCs. This process then inhibits the formation of the EGF receptor, thereby perturbing the EGF-mediated signaling that controls NPC proliferation and differentiation (Fig. 6).

The molecular mechanisms we identified are of significance to human health. There is a wide variation in choline intake in the diet; in several human cohorts choline intake varies by ~3-fold. The U.S. National Health and Nutrition Examination Survey (2009–2012) data showed that only 11% of adult Americans achieve the adequate intake levels of choline, with mean intake being 300 mg/d (10th percentile being 200 mg/d; 90th percentile being 500 mg/d) (56). Only 7% of women in the developed countries, and even fewer in the developing countries, achieve the recommended levels of choline intake (1, 8, 57–60). Moreover, almost half of women in North Carolina (USA) who could become pregnant had single nucleotide polymorphisms (SNPs) in the gene phosphatidylethanolamine *N*-methyltransferase, encoding an essential enzyme in the production of phosphatidylcholine in the liver (phosphatidylethanolamine *N*-methyltransferase), making these women sensitive to low dietary choline during pregnancy because they lacked the estrogen upregulation of phosphatidylethanolamine *N*-methyltransferase gene expression that is needed to meet the choline-demands of the growing fetus (61, 62). We demonstrated that reduction in choline supply during pregnancy leads to abnormalities in the cellular architecture of the developing cerebral cortex, potentially leading to cognitive deficits. Given that many women eat diets marginal in choline content during pregnancy, it is possible that what we call normal cognitive function in children is not optimal cognitive function. FJ

AUTHOR CONTRIBUTIONS

I. Trujillo-Gonzalez performed experiments, interpreted the data and wrote the manuscript; Y. Wang performed experiments; W. B. Friday performed experiments; K. C. Vickers and C. L. Toth performed experiments; L. Molina-Torres performed experiments; and N. Surzenko and S.H. Zeisel conceived the study, interpreted the data and wrote the manuscript.

REFERENCES

1. Zeisel, S. H. (2006) Choline: critical role during fetal development and dietary requirements in adults. *Annu. Rev. Nutr.* **26**, 229–250
2. Tayebati, S. K., Marucci, G., Santinelli, C., Buccioni, M., and Amenta, F. (2015) Choline-containing phospholipids: structure-activity relationships versus therapeutic applications. *Curr. Med. Chem.* **22**, 4328–4340
3. Meck, W. H., and Williams, C. L. (2003) Metabolic imprinting of choline by its availability during gestation: implications for memory and attentional processing across the lifespan. *Neurosci. Biobehav. Rev.* **27**, 385–399
4. Meck, W. H., and Williams, C. L. (1997) Perinatal choline supplementation increases the threshold for chunking in spatial memory. *Neuroreport* **8**, 3053–3059
5. Meck, W. H., Smith, R. A., and Williams, C. L. (1988) Pre- and postnatal choline supplementation produces long-term facilitation of spatial memory. *Dev. Psychobiol.* **21**, 339–353
6. Meck, W. H., Williams, C. L., Cermak, J. M., and Blusztajn, J. K. (2008) Developmental periods of choline sensitivity provide an ontogenetic mechanism for regulating memory capacity and age-related dementia. *Front. Integr. Nuerosci.* **1**, 7
7. Mellott, T. J., Williams, C. L., Meck, W. H., and Blusztajn, J. K. (2004) Prenatal choline supplementation advances hippocampal development and enhances MAPK and CREB activation. *FASEB J.* **18**, 545–547
8. Boeke, C. E., Gillman, M. W., Hughes, M. D., Rifas-Shiman, S. L., Villamor, E., and Oken, E. (2013) Choline intake during pregnancy and child cognition at age 7 years. *Am. J. Epidemiol.* **177**, 1338–1347
9. Shaw, G. M., Carmichael, S. L., Yang, W., Selvin, S., and Schaffer, D. M. (2004) Periconceptional dietary intake of choline and betaine and neural tube defects in offspring. *Am. J. Epidemiol.* **160**, 102–109
10. Craciunescu, C. N., Albright, C. D., Mar, M. H., Song, J., and Zeisel, S. H. (2003) Choline availability during embryonic development alters progenitor cell mitosis in developing mouse hippocampus. *J. Nutr.* **133**, 3614–3618
11. Wang, Y., Surzenko, N., Friday, W. B., and Zeisel, S. H. (2016) Maternal dietary intake of choline in mice regulates development of the cerebral cortex in the offspring. *FASEB J.* **30**, 1566–1578
12. Caric, D., Raphael, H., Viti, J., Feathers, A., Wancio, D., and Lillien, L. (2001) EGFRs mediate chemotactic migration in the developing telencephalon. *Development* **128**, 4203–4216
13. Burrows, R. C., Wancio, D., Levitt, P., and Lillien, L. (1997) Response diversity and the timing of progenitor cell maturation are regulated by developmental changes in EGFR expression in the cortex. *Neuron* **19**, 251–267
14. Ferri, R. T., and Levitt, P. (1995) Regulation of regional differences in the differentiation of cerebral cortical neurons by EGF family-matrix interactions. *Development* **121**, 1151–1160
15. Lillien, L., and Gulacsi, A. (2006) Environmental signals elicit multiple responses in dorsal telencephalic progenitors by threshold-dependent mechanisms. *Cereb. Cortex* **16**(Suppl 1), i74–i81
16. Wang, J., and Yu, R. K. (2013) Interaction of ganglioside GD3 with an EGF receptor sustains the self-renewal ability of mouse neural stem cells in vitro. *Proc. Natl. Acad. Sci. USA* **110**, 19137–19142
17. Fabian, M. R., Sonenberg, N., and Filipowicz, W. (2010) Regulation of mRNA translation and stability by microRNAs. *Annu. Rev. Biochem.* **79**, 351–379
18. Iwakawa, H. O., and Tomari, Y. (2015) The functions of MicroRNAs: mRNA decay and translational repression. *Trends Cell Biol.* **25**, 651–665
19. Bartel, D. P. (2004) MicroRNAs: genomics, biogenesis, mechanism, and function. *Cell* **116**, 281–297
20. Encinas, J. M., Vaahtokari, A., and Enikolopov, G. (2006) Fluoxetine targets early progenitor cells in the adult brain. *Proc. Natl. Acad. Sci. USA* **103**, 8233–8238
21. Lee, T. C., and Threadgill, D. W. (2009) Generation and validation of mice carrying a conditional allele of the epidermal growth factor receptor. *Genesis* **47**, 85–92
22. Madisen, L., Zwingman, T. A., Sunkin, S. M., Oh, S. W., Zariwala, H. A., Gu, H., Ng, L. L., Palmiter, R. D., Hawrylycz, M. J., Jones, A. R., Lein, E. S., and Zeng, H. (2010) A robust and high-throughput Cre reporting and characterization system for the whole mouse brain. *Nat. Neurosci.* **13**, 133–140
23. Lagace, D. C., Whitman, M. C., Noonan, M. A., Ables, J. L., DeCarolis, N. A., Arguello, A. A., Donovan, M. H., Fischer, S. J., Farnbauch, L. A., Beech, R. D., DiLeone, R. J., Greer, C. A., Mandyam, C. D., and Eisch, A. J. (2007) Dynamic contribution of nestin-expressing stem cells to adult neurogenesis. *J. Neurosci.* **27**, 12623–12629
24. Mehedint, M. G., Niculescu, M. D., Craciunescu, C. N., and Zeisel, S. H. (2010) Choline deficiency alters global histone methylation and epigenetic marking at the Re1 site of the calbindin 1 gene. *FASEB J.* **24**, 184–195
25. Scremin, O. U., Roch, M., Norman, K. M., Djazayeri, S., and Liu, Y. Y. (2015) Brain acetylcholine and choline concentrations and dynamics in a murine model of the Fragile X syndrome: age, sex and region-specific changes. *Neuroscience* **301**, 520–528
26. Yokota, Y., Ring, C., Cheung, R., Pevny, L., and Anton, E. S. (2007) Nap1-regulated neuronal cytoskeletal dynamics is essential for the final differentiation of neurons in cerebral cortex. *Neuron* **54**, 429–445
27. Yokota, Y., Kim, W. Y., Chen, Y., Wang, X., Stanco, A., Komuro, Y., Snider, W., and Anton, E. S. (2009) The adenomatous polyposis coli protein is an essential regulator of radial glial polarity and construction of the cerebral cortex. *Neuron* **61**, 42–56
28. Gstrein, T., Edwards, A., Přistoupilová, A., Leca, I., Breuss, M., Pilat-Carotta, S., Hansen, A. H., Tripathy, R., Traunbauer, A. K., Hochstoeger, T., Rosoklija, G., Repic, M., Landler, L., Stránecký, V., Dürnberger, G., Keane, T. M., Zuber, J., Adams, D. J., Flint, J., Honzik, T., Gut, M., Beltran, S., Mechtler, K., Sherr, E., Kmoch, S., Gut, I., and Keays, D. A. (2018) Mutations in Vps15 perturb neuronal migration in mice and are associated with neurodevelopmental disease in humans. *Nat. Neurosci.* **21**, 207–217; erratum: 1139
29. Lanaya, H., Natarajan, A., Komposch, K., Li, L., Amberg, N., Chen, L., Wculek, S. K., Hammer, M., Zenz, R., Peck-Radosavljevic, M., Sieghart, W., Trauner, M., Wang, H., and Sibilia, M. (2014) EGFR has a tumour-promoting role in liver macrophages during hepatocellular carcinoma formation. *Nat. Cell Biol.* **16**, 972–977
30. Molloy, A. M., Weir, D. G., Kennedy, G., Kennedy, S., and Scott, J. M. (1990) A new high performance liquid chromatographic method for the simultaneous measurement of S-adenosylmethionine and S-adenosylhomocysteine: concentrations in pig tissues after inactivation of methionine synthase by nitrous oxide. *Biomed. Chromatogr.* **4**, 257–260

31. John, B., Enright, A. J., Aravin, A., Tuschl, T., Sander, C., and Marks, D. S. (2004) Human MicroRNA targets. *PLoS Biol.* **2**, e363; erratum: 3, e264

32. Lewis, B. P., Shih, I. H., Jones-Rhoades, M. W., Bartel, D. P., and Burge, C. B. (2003) Prediction of mammalian microRNA targets. *Cell* **115**, 787–798

33. Zeisel, S. (2017) Choline, other methyl-donors and epigenetics. *Nutrients* **9**, 445

34. Davison, J. M., Mellott, T. J., Kovacheva, V. P., and Blusztajn, J. K. (2009) Gestational choline supply regulates methylation of histone H3, expression of histone methyltransferases G9a (Kmt1c) and Suv39h1 (Kmt1a), and DNA methylation of their genes in rat fetal liver and brain. *J. Biol. Chem.* **284**, 1982–1989

35. Tehlivets, O., Malanovic, N., Visram, M., Pavkov-Keller, T., and Keller, W. (2013) S-adenosyl-L-homocysteine hydrolase and methylation disorders: yeast as a model system. *Biochim. Biophys. Acta* **1832**, 204–215

36. Lupu, D. S., Orozco, L. D., Wang, Y., Cullen, J. M., Pellegrini, M., and Zeisel, S. H. (2017) Altered methylation of specific DNA loci in the liver of *Bhmt*-null mice results in repression of *Iqgap2* and *F2rl2* and is associated with development of preneoplastic foci. *FASEB J.* **31**, 2090–2103

37. Luan, Q. X., Zhang, B. G., Li, X. J., and Guo, M. Y. (2016) MiR-129-5p is downregulated in breast cancer cells partly due to promoter H3K27m3 modification and regulates epithelial-mesenchymal transition and multi-drug resistance. *Eur. Rev. Med. Pharmacol. Sci.* **20**, 4257–4265

38. Wu, Q., Yang, Z., Xia, L., Nie, Y., Wu, K., Shi, Y., and Fan, D. (2014) Methylation of miR-129-5p CpG island modulates multi-drug resistance in gastric cancer by targeting ABC transporters. *Oncotarget* **5**, 11552–11563

39. Lagos-Quintana, M., Rauhut, R., Yalcin, A., Meyer, J., Lendeckel, W., and Tuschl, T. (2002) Identification of tissue-specific microRNAs from mouse. *Curr. Biol.* **12**, 735–739

40. Gebhardt, M. L., Reuter, S., Mrowka, R., and Andrade-Navarro, M. A. (2014) Similarity in targets with REST points to neural and glioblastoma related miRNAs. *Nucleic Acids Res.* **42**, 5436–5446

41. Miska, E. A., Alvarez-Saavedra, E., Townsend, M., Yoshii, A., Sestan, N., Rakic, P., Constantine-Paton, M., and Horvitz, H. R. (2004) Microarray analysis of microRNA expression in the developing mammalian brain. *Genome Biol.* **5**, R68

42. Sosanya, N. M., Huang, P. P., Cacheaux, L. P., Chen, C. J., Nguyen, K., Perrone-Bizzozero, N. I., and Raab-Graham, K. F. (2013) Degradation of high affinity HuD targets releases Kv1.1 mRNA from miR-129 repression by mTORC1. *J. Cell Biol.* **202**, 53–69

43. Decembrini, S., Bressan, D., Vignali, R., Pitto, L., Mariotti, S., Rainaldi, G., Wang, X., Evangelista, M., Barsacchi, G., and Cremisi, F. (2009) MicroRNAs couple cell fate and developmental timing in retina. *Proc. Natl. Acad. Sci. USA* **106**, 21179–21184

44. Wu, J., Qian, J., Li, C., Kwok, L., Cheng, F., Liu, P., Perdomo, C., Kotton, D., Vaziri, C., Anderlind, C., Spira, A., Cardoso, W. V., and Lü, J. (2010) miR-129 regulates cell proliferation by downregulating Cdk6 expression. *Cell Cycle* **9**, 1809–1818

45. Zongaro, S., Hukema, R., D'Antoni, S., Davidovic, L., Barbry, P., Catania, M. V., Willemsen, R., Mari, B., and Bardoni, B. (2013) The 3′ UTR of FMR1 mRNA is a target of miR-101, miR-129-5p and miR-221: implications for the molecular pathology of FXTAS at the synapse. *Hum. Mol. Genet.* **22**, 1971–1982

46. Cremisi, F. (2013) MicroRNAs and cell fate in cortical and retinal development. *Front. Cell. Neurosci.* **7**, 141

47. Tropepe, V., Sibilia, M., Ciruna, B. G., Rossant, J., Wagner, E. F., and van der Kooy, D. (1999) Distinct neural stem cells proliferate in response to EGF and FGF in the developing mouse telencephalon. *Dev. Biol.* **208**, 166–188

48. Wagner, B., Natarajan, A., Grünaug, S., Kroismayr, R., Wagner, E. F., and Sibilia, M. (2006) Neuronal survival depends on EGFR signaling in cortical but not midbrain astrocytes. *EMBO J.* **25**, 752–762

49. Threadgill, D. W., Dlugosz, A. A., Hansen, L. A., Tennenbaum, T., Lichti, U., Yee, D., LaMantia, C., Mourton, T., Herrup, K., Harris, R. C., Barnard, J. A., Yuspa, S. H., Coffey, R. J., and Magnuson, T. (1995) Targeted disruption of mouse EGF receptor: effect of genetic background on mutant phenotype. *Science* **269**, 230–234

50. Sinor-Anderson, A., and Lillien, L. (2011) Akt1 interacts with epidermal growth factor receptors and hedgehog signaling to increase stem/transit amplifying cells in the embryonic mouse cortex. *Dev. Neurobiol.* **71**, 759–771

51. Close, J. L., Liu, J., Gumuscu, B., and Reh, T. A. (2006) Epidermal growth factor receptor expression regulates proliferation in the postnatal rat retina. *Glia* **54**, 94–104

52. Lillien, L., and Wancio, D. (1998) Changes in epidermal growth factor receptor expression and competence to generate glia regulate timing and choice of differentiation in the retina. *Mol. Cell. Neurosci.* **10**, 296–308

53. Reiter, J. L., Threadgill, D. W., Eley, G. D., Strunk, K. E., Danielsen, A. J., Sinclair, C. S., Pearsall, R. S., Green, P. J., Yee, D., Lampland, A. L., Balasubramaniam, S., Crossley, T. D., Magnuson, T. R., James, C. D., and Maihle, N. J. (2001) Comparative genomic sequence analysis and isolation of human and mouse alternative EGFR transcripts encoding truncated receptor isoforms. *Genomics* **71**, 1–20

54. Shyh-Chang, N., Locasale, J. W., Lyssiotis, C. A., Zheng, Y., Teo, R. Y., Ratanasirintrawoot, S., Zhang, J., Onder, T., Unternaehrer, J. J., Zhu, H., Asara, J. M., Daley, G. Q., and Cantley, L. C. (2013) Influence of threonine metabolism on S-adenosylmethionine and histone methylation. *Science* **339**, 222–226

55. Petrossian, T. C., and Clarke, S. G. (2011) Uncovering the human methyltransferasome. *Mol Cell Proteomics* **10**, M110.000976

56. Wallace, T. C., and Fulgoni III, V. L. (2016) Assessment of total choline intakes in the United States. *J. Am. Coll. Nutr.* **35**, 108–112

57. Wallace, T. C., McBurney, M., and Fulgoni III, V. L. (2014) Multivitamin/mineral supplement contribution to micronutrient intakes in the United States, 2007-2010. *J. Am. Coll. Nutr.* **33**, 94–102

58. Shaw, G. M., Carmichael, S. L., Laurent, C., and Rasmussen, S. A. (2006) Maternal nutrient intakes and risk of orofacial clefts. *Epidemiology* **17**, 285–291

59. Gossell-Williams, M., Fletcher, H., McFarlane-Anderson, N., Jacob, A., Patel, J., and Zeisel, S. (2005) Dietary intake of choline and plasma choline concentrations in pregnant women in Jamaica. *West Indian Med. J.* **54**, 355–359

60. Dominguez-Salas, P., Moore, S. E., Cole, D., da Costa, K. A., Cox, S. E., Dyer, R. A., Fulford, A. J., Innis, S. M., Waterland, R. A., Zeisel, S. H., Prentice, A. M., and Hennig, B. J. (2013) DNA methylation potential: dietary intake and blood concentrations of one-carbon metabolites and cofactors in rural African women. *Am. J. Clin. Nutr.* **97**, 1217–1227

61. Fischer, L. M., daCosta, K. A., Kwock, L., Stewart, P. W., Lu, T.-S., Stabler, S. P., Allen, R. H., and Zeisel, S. H. (2007) Sex and menopausal status influence human dietary requirements for the nutrient choline. *Am. J. Clin. Nutr.* **85**, 1275–1285

62. Resseguie, M. E., da Costa, K. A., Galanko, J. A., Patel, M., Davis, I. J., and Zeisel, S. H. (2011) Aberrant estrogen regulation of PEMT results in choline deficiency-associated liver dysfunction. *J. Biol. Chem.* **286**, 1649–1658